Non-local effects in dual-probe-sideband Brillouin optical time domain analysis

Alejandro Dominguez-Lopez,[1,*] Xabier Angulo-Vinuesa, [1] Alexia Lopez-Gil, [1] Sonia Martin-Lopez,[1] and Miguel Gonzalez-Herraez[1]

[1]*Departamento de Electrónica, Universidad de Alcalá. Escuela Politécnica Superior. Campus Universitario s/n. Alcala de Henares 28805, Spain.*
[*]*alejandro.dominguezl@uah.es*

Abstract: According to recent models, non-local effects in dual-probe-sideband Brillouin Optical Time Domain Analysis (BOTDA) systems should be essentially negligible whenever the probe power is below the Stimulated Brillouin Scattering (SBS) threshold. This paper shows that actually there appear non-local effects in this type of systems before the SBS threshold. To explain these effects it is necessary to take into account a full spectral description of the SBS process. The pump pulse experiences a frequency-dependent spectral deformation that affects the readout process differently in the gain and loss configurations. This paper provides a simple analytical model of this phenomenon, which is validated against compelling experimental data, showing good agreement. The main conclusion of our study is that the measurements in gain configuration are more robust to this non-local effect than the loss configuration. Experimental and theoretical results show that, for a total probe wave power of ~1 mW (500 μW on each sideband), there is an up-shifting of ~1 MHz in the Brillouin Frequency Shift (BFS) retrieved from the Brillouin Loss Spectrum, whereas the BFS extracted from the measured Brillouin Gain Spectrum is up-shifted only ~0.6 MHz. These results are of particular interest for manufacturers of long-range BOTDA systems.

OCIS codes: (290.5900) Scattering, stimulated Brillouin; (290.5830) Scattering, Brillouin; (060.2370) Fiber optics sensors; (060.4370) Nonlinear optics, fibers.

References and links

1. M. Niklès, L. Thévenaz, and P. A. Robert, "Simple distributed fiber sensor based on Brillouin gain spectrum analysis," Opt. Lett. **21**(10), 758–760 (1996).
2. M. Niklès, "Long-distance fiber optic sensing solutions for pipeline leakage, intrusion, and ground movement detection," Proc. SPIE **7316**, 731602, 731602-13 (2009).
3. T. Horiguchi and M. Tateda, "Optical-fiber-attenuation investigation using stimulated Brillouin scattering between a pulse and a continuous wave," Opt. Lett. **14**(8), 408–410 (1989).
4. T. Horiguchi and M. Tateda, "BOTDA-Nondestructive measurement of single-mode optical fiber attenuation characteristics using Brillouin interaction: Theory," J. Lightwave Technol. **7**(8), 1170–1176 (1989).
5. M. Niklès, L. Thévenaz, and P. A. Robert, "Brillouin Gain Spectrum Characterization in Single-Mode Optical Fibers," J. Lightwave Technol. **15**(10), 1842–1851 (1997).
6. G. P. Agrawal, "Stimulated Brillouin Scattering," in *Nonlinear Fiber Optics, 3rd ed.* (Academic, 2001) pp. 355–384.
7. L. Thévenaz, S. F. Mafang, and J. Lin, "Effect of pulse depletion in a Brillouin optical time-domain analysis system," Opt. Express **21**(12), 14017–14035 (2013).
8. A. Minardo, R. Bernini, and L. Zeni, "A simple technique for reducing pump depletion in long-range distributed Brillouin fiber sensors," IEEE Sens. J. **9**(6), 633–634 (2009).
9. J. Urricelqui, M. Sagues, and A. Loayssa, "Phasorial differential pulse-width pair technique for long-range Brillouin optical time-domain analysis sensors," Opt. Express **22**(14), 17403–17408 (2014).
10. A. Loayssa, R. Hernández, D. Benito, and S. Galech, "Characterization of stimulated Brillouin scattering spectra by use of optical single-sideband modulation," Opt. Lett. **29**(6), 638–640 (2004).
11. A. Domínguez-López, A. López-Gil, S. Martín-López, and M. González-Herráez, "Signal-to-noise ratio improvement in BOTDA using balanced detection," IEEE Photon. Technol. Lett. **26**(4), 338–341 (2014).

#231569 - $15.00 USD Received 16 Jan 2015; revised 23 Mar 2015; accepted 25 Mar 2015; published 14 Apr 2015

12. A. Domínguez-López, A. López-Gil, S. Martín-López, and M. González-Herráez, "Strong cancellation of RIN transfer in a Raman-assisted BOTDA using balanced detection," IEEE Photon. Technol. Lett. **26**(18), 1817–1820 (2014).
13. J. P. Gordon, "Theory of the soliton self-frequency shift," Opt. Lett. **11**(10), 662–664 (1986).

1. Introduction

Brillouin-based distributed temperature and strain sensors are extremely attractive in civil engineering thanks to their unique capabilities to monitor large linear infrastructures [1, 2]. In particular, Brillouin optical time-domain analysis (BOTDA) systems are nowadays extensively used for the surveillance of different critical assets including pipelines, umbilical cables, bridges, etc.

BOTDA schemes rely on mapping the Stimulated Brillouin Scattering (SBS) characteristics along the length of an optical fiber [3–5]. When an intense coherent beam is introduced in the fiber, SBS leads to the generation of two spectral signatures in the counter-propagating direction: a frequency down-shifted gain spectrum (Stokes band) and a frequency up-shifted attenuation spectrum (anti-Stokes band) [6]. The interrogation of this process in a distributed manner requires the use of two different counter-propagating light beams in the fiber. One of the light beams (pump) is pulsed and is meant to generate some amplification/attenuation on the counter-propagating continuous-wave beam (probe). As the pump pulse travels along the fiber, it will induce a different amplification/attenuation on the probe, depending on the local Brillouin Frequency Shift (BFS) and the pump-probe frequency difference. The local amplification/attenuation of the probe wave yields a time-dependent variation of the detected probe signal at the pump end, which is translated into positional information using the time of flight of the pulse. The gain/loss at each point is maximized when the pump-probe frequency separation matches exactly the BFS at that position. By scanning for this maximum at all the positions, one can obtain a map of the BFS of the fiber across its whole length.

The basic assumption of the measurement technique is that the power lost or gained by the pump pulse through SBS is negligible in comparison to the total pulse power [7]. This is the only way to ensure that strictly local information is retrieved from the variations of the probe beam. Non-local effects in these systems appear when the integrated power transfer from pump to probe is non-negligible in comparison to the total pump power. These situations are of important concern, as they cause deformations of the observed Brillouin gain/loss curves, which lead to errors in the determination of the BFS as a function of the position. The exact error introduced depends on the whole BFS landscape of the fiber, and this is why these impairments in the measurement are termed as "non-local effects". Strategies to avoid non-local effects have been put forward in the literature [8, 9].

In BOTDA systems, pump and probe waves are usually developed from a single laser source using RF modulation [1]. This allows a very stable interrogation system where the pump-probe frequency difference is solely determined by the RF modulation frequency, regardless of the master laser drifts. Single-sideband [10] (SSB) or dual-sideband [8] (DSB) probe modulations are conventionally employed. In single-sideband modulation, the resulting probe is tuned to either the gain band or the loss band of the SBS process. It has the advantage of requiring less filtering elements in the optical path, but non-local effects can adversely affect it. In dual-sideband modulation, two perfectly symmetric sidebands are created: one scans the gain region and the other scans the loss region. The advantage of this configuration is that the power lost by the pump in the gain process is essentially recovered in the loss process. Thus, overall, depletion (or non-local) effects are strongly mitigated. The use of DSB modulation to generate the probe wave has therefore become a widespread solution in the past few years. Moreover, it can be fully exploited if balanced detection [11, 12] is used upon reception.

According to recent models [7], non-local effects in DSB systems should be largely negligible up to the limit of SBS threshold of the probe signal. These models take root on a "quasi-cw" assumption on the pump pulse. While this is a correct assumption in most cases, it may lead to an incomplete description of the non-local effects in this situation. The work

#231569 - $15.00 USD Received 16 Jan 2015; revised 23 Mar 2015; accepted 25 Mar 2015; published 14 Apr 2015

presented in this paper shows that to understand non-local effects in this case, a full spectral description of the process is necessary. The rest of the paper is structured as follows: section 2 provides a theoretical analysis of non-local effects in a DSB BOTDA together with the mathematical model used in this paper. Section 3 provides details on the experimental setup used to show these effects and section 4 provides the results obtained, comparing theory and experimental results. Finally, the last section explains the conclusions of this study.

2. Theoretical analysis

When using DSB modulation, the higher frequency sideband of the probe (that scans the Brillouin Loss process) provides power to the pump pulse, and at the same time, the pump pulse provides power to the lower frequency probe sideband (that scans the Brillouin Gain). This situation can be analyzed in the analogous way in which the higher and lower frequency sidebands of the probe generate, respectively, a gain and a loss around the pump frequency. Depending on the modulation frequency, the relative position of the gain and loss signatures and the pump pulse can be different, as shown in Fig. 1.

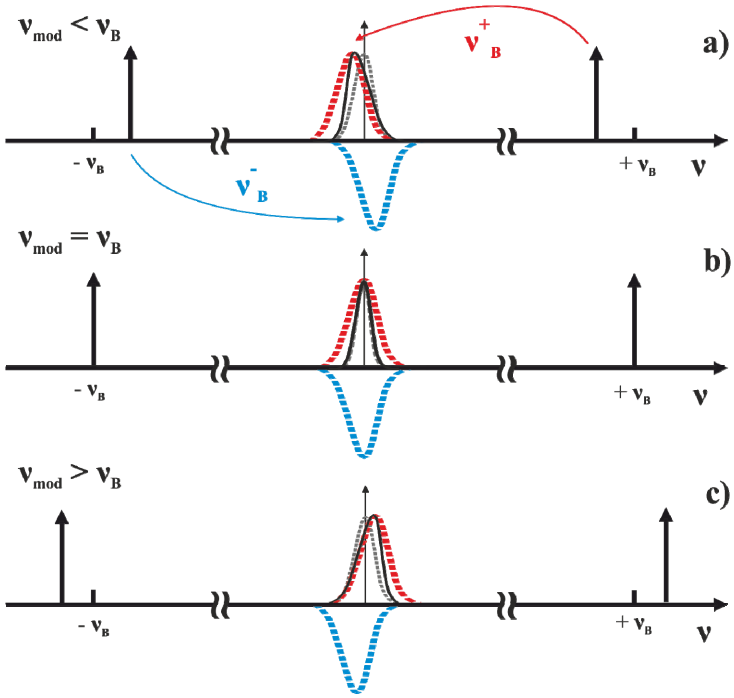

Fig. 1. Illustration of the SBS-induced distortion in the pump pulse when using DSB-SC modulation on the probe wave. The pump pulse suffers a spectral deformation with several consequences, including a spectral deformation and a shifting of the central frequency.

When the probe wave is modulated to match the Brillouin Frequency Shift (BFS) ($\nu_{mod} = \nu_B$), the amplification and attenuation processes generated, respectively, by the upper and lower frequency sidebands, will occur at the pump frequency, as shown in Fig. 1(b). This leads to an essentially undistorted pulse spectrum along the distance. However, modulation of the probe wave at a frequency below the BFS [Fig. 1(a)] ($\nu_{mod} < \nu_B$) implies an amplification curve occurring at a frequency lower than the pump frequency, and simultaneously, an attenuation process happening at a frequency above the pump frequency (note that the amplification and attenuation processes manifest at a frequency shifted $\pm \nu_B$ from the corresponding probe frequency). The overall result is that the pump pulse is spectrally distorted and down-shifted, in a similar way as the Raman frequency shift of solitons [13]. On the other hand, when the modulation frequency is above the BFS [Fig. 1(c)] ($\nu_{mod} > \nu_B$), the amplification process generated by the upper frequency sideband occurs at a higher frequency

#231569 - $15.00 USD Received 16 Jan 2015; revised 23 Mar 2015; accepted 25 Mar 2015; published 14 Apr 2015

than the pump frequency, and equivalently, the attenuation generated by the lower frequency band occurs at a lower frequency than the pump frequency. This will again lead to a distortion of the pulse spectrum and an up-shifting of its central frequency. Thus, sweeping the modulation frequency around the BFS will modify the pump pulse spectrum, turning it asymmetrical and spectrally shifted upwards or downwards depending on whether the modulation frequency is higher or lower than the BFS. This has a strong impact on how the gain and loss curves are retrieved as we will see next.

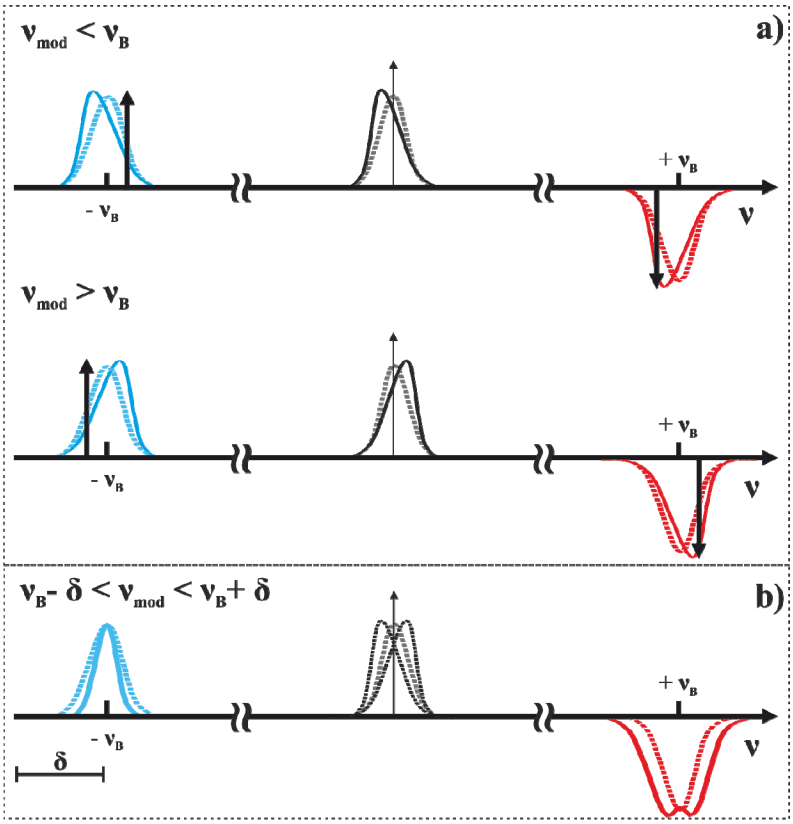

Fig. 2. a) Illustration of the SBS interaction between a non-uniform pulse spectrum and the Brillouin Gain and Loss curves while sweeping the probe wave modulation frequency; b) Resulting spectra after a complete sweep of the probe wave modulation frequency, varying such frequency over a certain amount (± δ) around the BFS of the FUT. The gain process shows an apparent narrowing while the attenuation process appears to be broader.

When performing BOTDA measurements, a frequency sweep around the BFS is needed on the probe wave modulation in order to recover a complete BFS profile of the Fiber Under Test (FUT). Therefore, changing the probe wave frequency, the Brillouin Gain and Loss curves interact with a pump pulse spectrum that is spectrally different for each probe frequency, as illustrated in Fig. 2. In particular, when the modulation frequency is below the BFS, the pulse central frequency is down-shifted. This implies that the new frequency difference among pump and upper sideband is closer to the BFS (thus the attenuation is overestimated) and conversely, the frequency difference among pump and lower frequency probe band is lower, which implies an underestimation of the gain curve. A similar situation can be observed in the case in which the modulation frequency is above the BFS [Fig. 2(b)]. In this case the pulse central frequency is up-shifted, which implies that the new frequency difference among pump and upper sideband is closer to the BFS. Again, in this situation, the attenuation is overestimated and the gain is underestimated.

#231569 - $15.00 USD Received 16 Jan 2015; revised 23 Mar 2015; accepted 25 Mar 2015; published 14 Apr 2015

This particular phenomenon leads to one remarkable result: as the pump pulse advances towards the end of the fiber, the "observed" Brillouin Gain Spectrum (BGS) progressively narrows while the observed Brillouin Loss Spectrum (BLS) broadens. Such important outcome will imply a better determination of the BFS in the Brillouin Gain case and a worse determination in the Brillouin Loss one. Moreover, it can be shown that the energy content of the pulse grows slightly when the modulation frequency is slightly detuned from the BFS. This behavior is responsible for the appearance of two side lobes in the Brillouin Loss curve. These results will be discussed in detail in section 4. As we will see, the appearance of undesired lobes is proportional to the probe wave power provided at the fiber end.

There is an additional point of concern for BOTDA developers in this case, which has to do with the fact that the Brillouin gain and loss processes on the pump induced by, respectively, the upper and lower frequency sidebands of the probe are not exactly located at the same frequency offset from their corresponding sideband. Indeed, the differences in Brillouin shift between the processes generated by the upper and lower sidebands is given by:

$$\nu_B^+ - \nu_B^- = \frac{2nV_A}{\lambda_{us}} - \frac{2nV_A}{\lambda_{ls}} \tag{1}$$

Where λ_{us} and λ_{ls} are respectively, the upper and lower frequency sidebands, n is the refractive index of the fiber and V_A is the acoustic velocity in the fiber. A rapid evaluation of this quantity yields a frequency offset between both processes of ~1.2 MHz in typical conditions. As we will see in the detailed modeling, this induces some asymmetry in the spectral deformation of the pulse described above. In particular, we will see that the BFS estimation tends to be increasingly overestimated as a function of the distance. This effect, although small, is non-negligible.

To model this effect mathematically we will assume that the probe waves experience simple linear attenuation along the fiber. In addition, for now on, we will consider pump pulses with a duration longer than the phonon lifetime (pulse width >> 10 ns). The evolution of pump power with the distance z is then given by:

$$dP_P(\nu,z) = -\alpha P_P(\nu)\,dz + \left[g_B\left(\nu,\nu_{\text{mod}} - \nu_B^+\right) - g_B\left(\nu,\nu_B^- - \nu_{\text{mod}}\right)\right] P_s(z) P_P(\nu,z)\,dz \tag{2}$$

Where ν is the modulation frequency, α is the attenuation, P_P is the peak pump power and P_S is the probe wave power (where $P_s \equiv P_{us} \equiv P_{ls}$, P_{us} and P_{ls} being the probe power in the upper and lower sideband, respectively). $g_B(\nu,\nu_B)$ is the Lorentzian Brillouin gain profile as a function of the offset frequency ν, given by the following expression:

$$g_B(\nu,\nu_B) = \frac{g_B}{1 + \dfrac{(\nu - \nu_B)^2}{\left(\dfrac{\Delta\nu_B}{2}\right)^2}} \tag{3}$$

The pump spectrum as a function of the distance can be solved now:

$$P_P(\nu,z)\big|_{\nu_{\text{mod}}} =$$

$$= P_P(\nu,0)\exp(-\alpha z)\exp\left[\left(g_B\left(\nu,\nu_{\text{mod}} - \nu_B^+\right) - g_B\left(\nu,\nu_B^- - \nu_{\text{mod}}\right)\right) P_s(L)\exp(-\alpha L)\frac{\exp(\alpha z) - 1}{\alpha}\right] \tag{4}$$

At each position, the actual gain spectrum observed will be the natural (Lorentzian) gain spectrum convolved with the pump spectrum:

$$g(\nu,z)\big|_{\nu_{\text{mod}}} = g_B(\nu,\nu_B) \otimes P_P(\nu,z)\big|_{\nu_{\text{mod}}} \tag{5}$$

For each probe frequency, this spectrum is read at the corresponding modulation frequency (ν_{mod}), thus, evaluating the gain spectrum obtained in Eq. (5) for $\nu = \nu_{\text{mod}}$.

#231569 - $15.00 USD Received 16 Jan 2015; revised 23 Mar 2015; accepted 25 Mar 2015; published 14 Apr 2015

Correspondingly, the same process is followed to compute the loss spectrum and the recovered BLS value at $\nu = -\nu_{mod}$. Note that each modulation frequency yields a different pump deformation, and therefore the gain value read has to be recalculated for each case.

To further clarify such phenomenon, an illustration of the pulse shifting and asymmetrization process is shown in Fig. 3 for different values of ν_{mod}. The frequency displacement and the spectral disproportion turns out to be non-negligible when sweeping the modulation frequency around the BFS of the fiber.

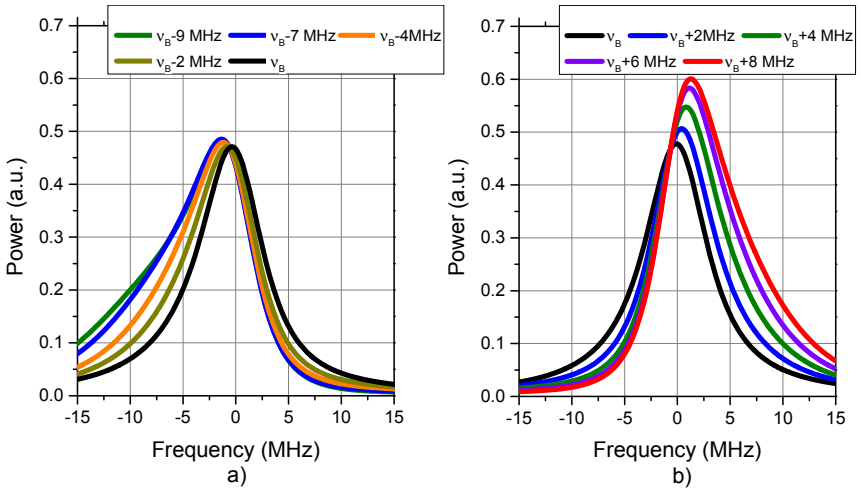

Fig. 3. Pump pulse theoretical spectra after going through the fiber and interacting with a probe wave whose modulation frequency is sweeping around the BFS of the FUT. a) Sweeping frequency below the BFS; b) Sweeping frequency above the BFS.

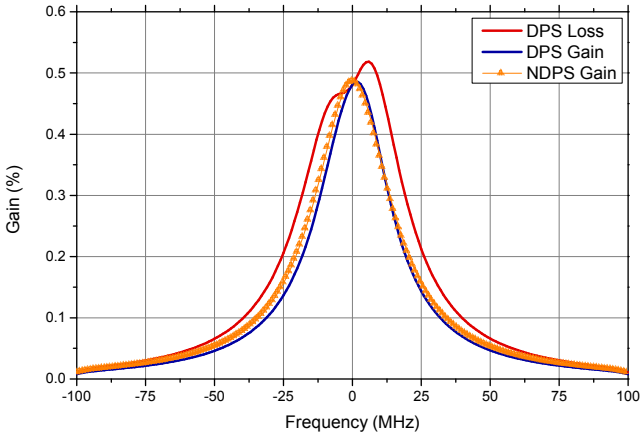

Fig. 4. Simulated BGS and BLS retrieved for a distorted pulse spectrum (DPS) overlapped with the simulated BGS for a non-distorted pulse spectrum (NDPS) at the end of the FUT for a pump pulse peak power of ~57 mW and a probe wave power of ~275 μW (on each sideband). Simulations obtained for a Gaussian pump pulse of 10 MHz of width.

Furthermore, a simulation of the interaction between a spectrally non-uniform pump pulse and a probe wave whose modulation frequency varies around the BFS has been carried out. Figure 4 illustrates the calculated BGS and BLS at the end of the fiber, where the BLS starts to show two undesired side lobes around the center frequency of the curve meanwhile the BGS remains well-proportioned and similar to the expected value. Besides such disproportion, the BGS presents a narrower profile than the BLS, which could lead to a better

#231569 - $15.00 USD Received 16 Jan 2015; revised 23 Mar 2015; accepted 25 Mar 2015; published 14 Apr 2015

determination of the BFS extracted from the BGS compared to the BLS case. Moreover, both gain and loss curves are slightly up-shifted in comparison with the expected curve for the BFS at that position. This shift is usually in the order of 1 MHz or below 1 MHz, so comparable to the usual values of uncertainty. These consequences, among others, will be studied in further detail in the forthcoming sections.

3. Experimental setup

To prove the above model of non-local effects in DSB BOTDA systems, we developed the BOTDA scheme represented in Fig. 5. It is a variation of the classical BOTDA system prepared by this group [11] but generating the pump pulse using an Electro-Optical Modulator (EOM) and a conventional single-sideband detection scheme.

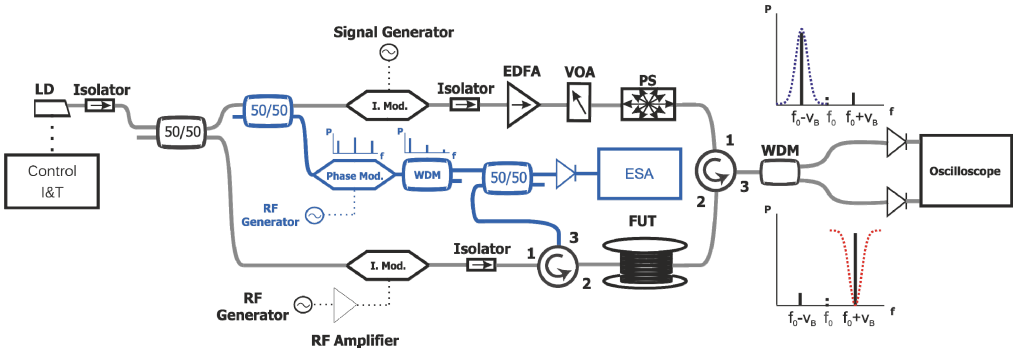

Fig. 5. BOTDA experimental setup. LD: Laser Diode; I. Mod.: Intensity Modulator; EDFA: Erbium Doped Fiber Amplifier; RF: Radio-frequency generator; VOA: Variable Optical Attenuator; PS: Polarization Scrambler; FUT: Fiber Under Test; WDM: Wavelength Division Multiplexer; ESA: Electrical Spectrum Analyzer.

As in most BOTDA setups, pump and probe waves are developed from a single distributed feed-back (DFB) laser diode. A Mach-Zehnder EOM is used to make a dual sideband with suppressed carrier (DSB-SC) modulation in the probe. The extinction ratio of the EOM is >40 dB, thus it is possible to nearly eliminate the carrier signal. The probe power fed into the fiber is ~500 μW on each sideband. The modulation frequency of the EOM is controlled through an RF Generator. The RF frequency is chosen to sweep around the BFS of the FUT.

At the pump side, the signal is pulsed using another EOM. The EOM allows to shape high extinction ratio (~30 dB) optical pulses. The pulse widths used in the experiment are 50 ns, which implies a 5 meter spatial resolution. The pulses are then amplified through an Erbium Doped Fiber Amplifier (EDFA), and their power is controlled through a Variable Optical Attenuator (VOA). After the VOA, their polarization is scrambled by a fast polarization scrambler. The peak power of the pulses fed into the fiber is ~50 mW.

After going through the fiber and experiencing Brillouin Scattering, the probe sidebands are separated using a conventional 100 GHz dense wavelength division multiplexing (DWDM) filter. The edge of the filter used is sharp enough to separate both sidebands correctly, attenuating the rejected band in >13 dB. The Brillouin Gain (Stokes) and Loss (anti-stokes) bands are then fed into two equal photodetectors, so as to acquire both signals simultaneously.

In addition, in order to check the spectral evolution of the pump pulse along the fiber, we have used an extra setup in order to self-heterodyne the pulse. First of all, we split the master laser again using a 50/50 coupler. While one of the arms is used to shape the pump, the other is phase-modulated by means of an Electro-Optical Phase Modulator at a certain RF frequency. The RF frequency is set using an external RF Generator. The lower sideband of the resulting modulated wave is selected by means of a DWDM filter. An optical circulator is placed at the end of the FUT, on the probe side, so we can recover the pulse after interacting

#231569 - $15.00 USD Received 16 Jan 2015; revised 23 Mar 2015; accepted 25 Mar 2015; published 14 Apr 2015

with the probe sidebands through SBS. This pulse is then recombined with the selected sideband of the phase modulation, and the resulting combination is fed into a high bandwidth photodetector. This allows us to observe the pulse spectral shifting/deformation with high spectral resolution and capability to discriminate the sense of the frequency shifts.

4. Results

We are now ready to take a deeper look at the results obtained with the developed setup. The measurements have been performed over ~50 km of single-mode fiber (SMF) with an essentially homogeneous BFS located at 10.865 GHz at the pump wavelength (~1550 nm). The acquired traces have always been averaged 1024 times.

The first remarkable result is the observation of an asymmetric spectral shift of the pump pulse dependent on the probe frequency. In Fig. 6 we can see the evolution of the electrical spectrum of the pump pulse after experiencing SBS through the fiber. A 32 GHz bandwidth Electrical Spectrum Analyzer (ESA) has been used to acquire a probe frequency sweep for a fixed probe power. As it can be seen (and as expected in the qualitative model of section 2), the interaction of both the attenuation and amplification processes with the pulse modifies its spectral shape, leading to an upshifting of the pulse when the modulation frequency is above ν_B and a down shifting when it is below. Moreover, the separation from the BFS frequency also leads to an increase in the pulse energy content, which is larger when the modulation frequency is above the BFS. As previously discussed, the slight offset among BFSs generated by the upper and lower modulation bands unbalances the power provided for the same probe frequency separation from the BFS.

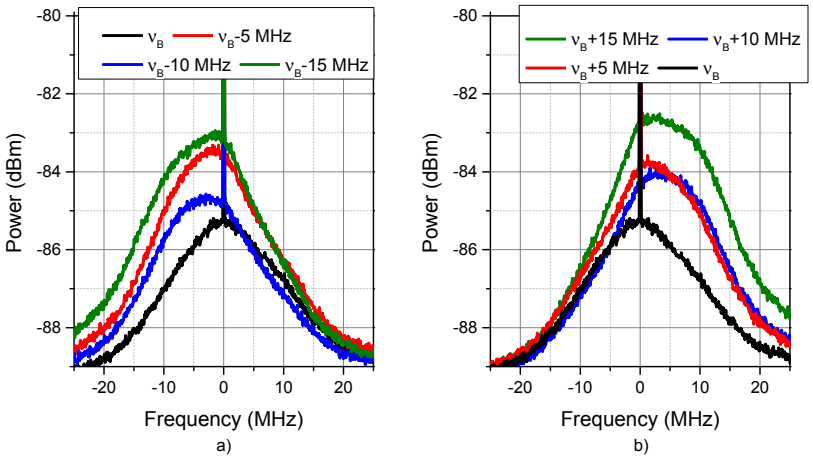

Fig. 6. Electrical spectra (75 kHz of resolution bandwidth) of the detected pump pulse recorded after going through the FUT and experiencing SBS for a fixed probe wave power of ~500 μW (on each sideband), sweeping the probe modulation frequency around the BFS of the FUT; a) Sweeping frequency below the BFS; b) Sweeping frequency above the BFS. The vertical lines located at 0 MHz in the spectra correspond to the DC leakage of the pump pulse.

In Fig. 7, the same analysis has been carried out but fixing the probe frequency and varying the probe power delivered into the fiber. Such analysis illustrates that the more powerful the probe wave is, the more asymmetrical the pulse shape becomes. It can be observed that even for the less powerful case, the pulse spectrum remains slightly asymmetrical.

#231569 - $15.00 USD Received 16 Jan 2015; revised 23 Mar 2015; accepted 25 Mar 2015; published 14 Apr 2015

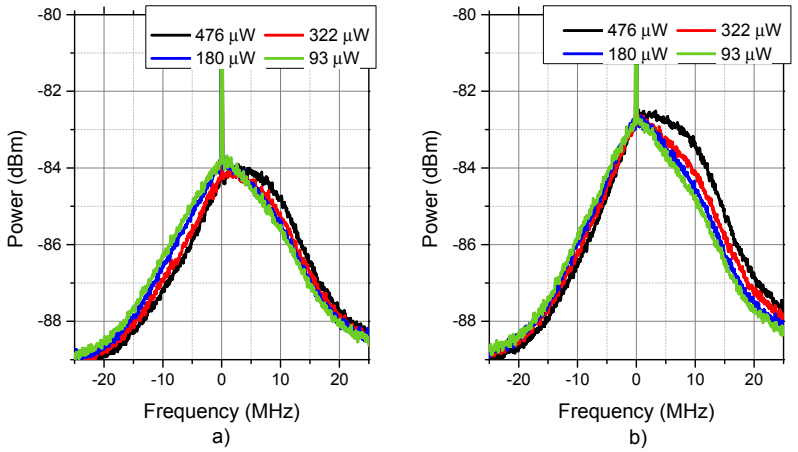

Fig. 7. Electrical spectra (75 kHz of resolution bandwidth) of the detected pump pulse recorded after going through the FUT and experiencing. a) Probe power variation for a fixed probe wave modulation frequency of 10.873 GHz (νB + 5 MHz). b) Probe power variation for a fixed probe wave modulation frequency of 10.873 GHz (νB + 10 MHz). Again, the vertical lines located at 0 MHz in the spectra correspond to the DC leakage of the pump pulse.

As we pointed out previously, such remarkable phenomenon leads us to a major outcome: it broadens and distorts the BLS profile meanwhile narrows the BGS. Figure 8 shows the theoretical and experimental BLS and BGS analysis for a probe wave of ~500 µW (on each sideband); Fig. 8(a) represents both the BGS and BLS at a distance of 49.768 km; Fig. 8(b) illustrates the evolution of the Full Width at Half Maximum (FWHM) of the BGS and BLS profiles along the distance. As it can be seen, the FWHM of the experimental BLS broadens ~7.5 MHz, meanwhile the simulated results show a broadening of ~8.5 MHz. Conversely, the FWHM of the BGS narrows ~3 MHz, confirming the decrease of ~3 MHz observed at the simulated results.

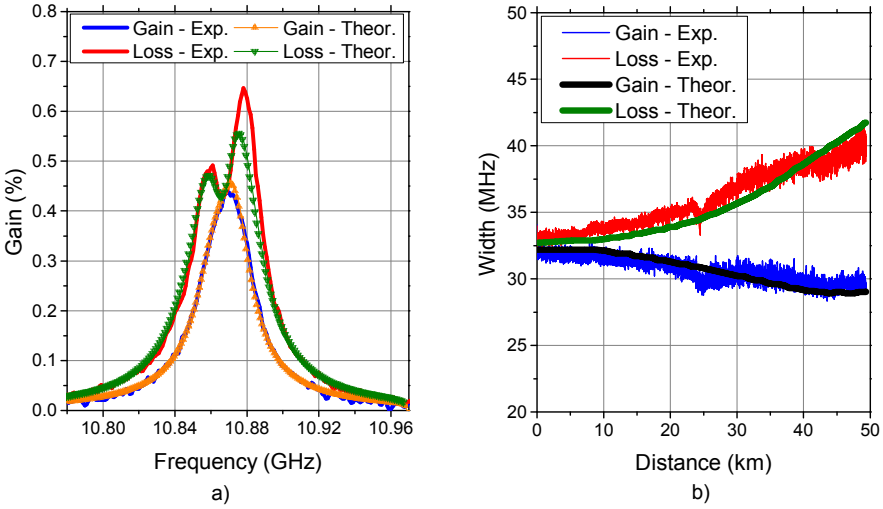

Fig. 8. BOTDA outcomes for a probe wave power of ~500 µW (on each sideband). a) Experimental and theoretical representation of the BGS and BLS at 49.768 km for a frequency sweep between 10.78 GHz and 10.98 GHz. b) Experimental and theoretical evolution of the FWHM for the Brillouin Gain and Brillouin Loss spectra.

In Fig. 8(a), we can see the Gain and Loss spectra for a probe power of ~500 µW (on each sideband) at the very end of the FUT (point 49.768 km). The measured distorted BLS and

#231569 - $15.00 USD Received 16 Jan 2015; revised 23 Mar 2015; accepted 25 Mar 2015; published 14 Apr 2015

BGS curves are well recovered by the model as we can see. The spurious new lobes retrieved on the BLS are, in fact, as predicted, slightly unbalanced among each other due to the small BFS offset generated by the Brillouin Gain and Loss bands. In this case, the theoretical model adjusts correctly to the experimental result, following reliably the profile shape.

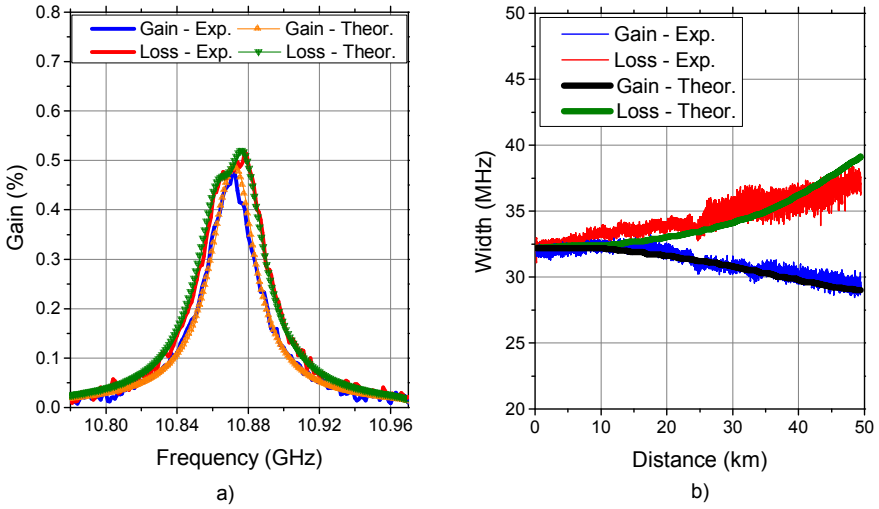

Fig. 9. BOTDA analysis for a probe wave power of ~275 μW (on each sideband). a) Experimental and theoretical representation of the BGS and BLS at 49.768 km for a frequency sweep between 10.78 GHz and 10.98 GHz. b) Experimental and theoretical evolution of the FWHM for the Brillouin Gain and Brillouin Loss spectra.

The same analysis has been now carried out reducing the probe wave power to ~275 μW on each sideband. As Fig. 9(a) illustrates, the disproportion and the spurious side lobes have decreased at the same time the probe power has been reduced. Such outcome confirms the theoretical analysis studied in previous sections (the experimental data profiles follow precisely the theoretical curves). The FWHM of the BGS continues to be narrower than the BLS one. Analyzing the evolution of the FWHM of both the BGS and BLS along the fiber [Fig. 9(b)], the FWHM of the BLS tends to be wider at the end of the fiber meanwhile the width of the BGS narrows towards the end of it. In particular, the FWHM of the experimental BLS broadens ~5 MHz, meanwhile the simulated results show a broadening of ~7 MHz. On the other hand, the FWHM of the BGS narrows ~3 MHz, once again, verifying the ~3 MHz decrease observed at the simulated results.

On top of the above results, we have taken a deeper look at the consequences of these non-local effects in terms of the BFS determination. As we have already seen, the BLS at the very end of the fiber presents two asymmetric side lobes [see Fig. 8(a)]. Indeed, due to the small mismatch of the BFS generated by the Brillouin Gain and Loss bands, such spurious peaks are unequal, and the higher frequency lobe always prevails over the lower frequency one. The appearance of these lobes can lead to a distorted determination of the maximum of the retrieved curves, which should be consistently overestimated.

In Fig. 10 we analyze the mismatch in the determination of the BFS along the fiber when increasing the probe power (hence increasing the asymmetry in the side lobes). Figure 10(a) illustrates the BFS profile of the Brillouin Gain spectrum along the fiber for two different probe wave powers. Increasing the probe wave power leads to a BFS displaced an average of ~0.6 MHz to higher frequencies at the very end of the fiber. On the contrary, the BFS obtained from the Brillouin Loss spectrum [Fig. 10(b)] shifts ~1 MHz to higher frequencies when strengthening the asymmetry of the pump pulse spectrum. Furthermore, we have also observed the behavior of the BFS obtained for both the BGS and BLS for a fixed probe wave power [Fig. 10(c)]. The displacement of the BFS extracted from the measured loss curve at the very end of the fiber is again ~1 MHz above the BFS obtained in the gain case, whereas

#231569 - $15.00 USD Received 16 Jan 2015; revised 23 Mar 2015; accepted 25 Mar 2015; published 14 Apr 2015

the BFS measured for both cases at the beginning of the FUT remains equal. These results clearly confirm the slight up-shifting phenomenon of the BFS predicted by the qualitative models, which is stronger in the attenuation case.

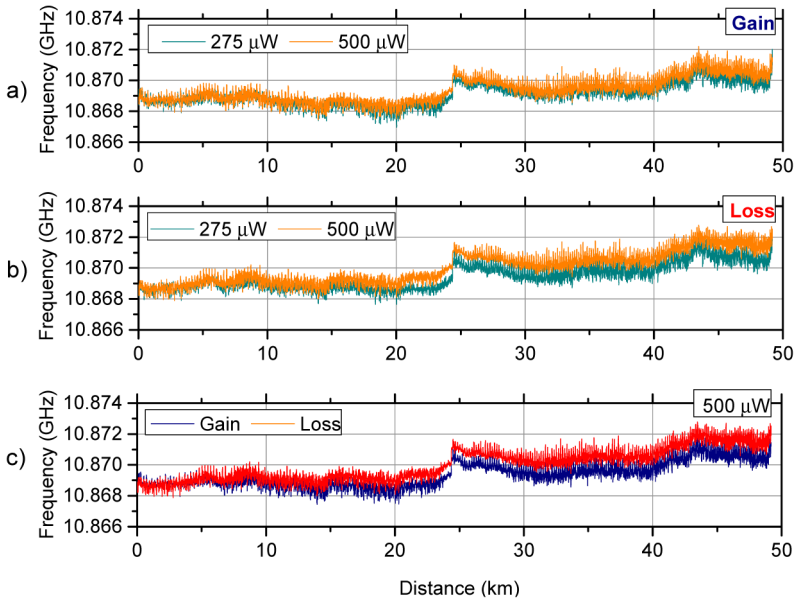

Fig. 10. Brillouin frequency shift profiles obtained for different probe wave powers on a ~50 km SMF. a) BFS profiles obtained from the measured Brillouin Gain band for two values of probe power; b) BFS profiles obtained from the measured Brillouin Loss band for two values of probe power; c) BFS profiles of the Brilluoin Gain and Loss bands for a fixed probe wave power of ~500 μW (on each sideband).

5. Conclusions

In conclusion, we have presented a series of non-local effects of dual-probe-sideband BOTDA systems, which, to our knowledge, had not been described before, and the consequences of them. The pump pulse changes severely its spectral shape when varying the probe wave modulation frequency. These spectral changes manifest as a shift and an asymmetric energy growth depending on the exact detuning from the BFS frequency. Such asymmetry is directly related to the power of the probe beam employed, so the more powerful the probe wave is, the more asymmetrical the pulse spectra become.

When performing BOTDA measurements, the interaction between a probe beam and a spectrally non-uniform pump pulse provokes distorted Brillouin Gain and Loss curves. The most remarkable consequence of this phenomenon is that the Full Width at Half Maximum (FWHM) of the Brillouin Gain Spectrum (BGS) narrows towards the end of the fiber, whereas the FWHM of the Brillouin Loss Spectrum (BLS) considerably broadens. Besides, the BLS is affected by the appearance of spurious side lobes meanwhile the BGS remains roughly well-proportioned.

In addition, the slight offset among the gain and loss processes generated by the upper and lower frequency components of the probe creates an asymmetry in the retrieved BGS and BLS curves that yields in an error in the determination of the BFS. In both cases, the BFS tends to shift to higher frequencies towards the end of the fiber, being larger the error in the attenuation case. All the undesired effects mainly prevail in the Brillouin Loss case over the Gain one. All these results have been demonstrated both theoretically and experimentally.

We also envisage that the spectral deformation of the pump pulse might affect the spatial resolution of the system. Indeed, for high probe powers, and depending on the modulation frequency, a substantial spectral deformation is visible (including spectral broadening in some

#231569 - $15.00 USD Received 16 Jan 2015; revised 23 Mar 2015; accepted 25 Mar 2015; published 14 Apr 2015

cases), which could be associated to temporal distortion in the pulse. Moreover, although this study refers to the appearance of these non-local effects in dual-probe-sideband BOTDA, we foresee that this frequency-dependent phenomenon described in the paper will also appear in a single-sideband (SSB) BOTDA scenario. Hence, we believe all these results may have important implications for developers of long-range BOTDA systems.

Acknowledgments

This work was supported in part by the European Research Council through U-FINE under Grant 307441, in part by the Spanish Ministry of Science and Innovation under Projects TEC2012-37958-C02-01, TEC2012-37958-C02-02 and TEC2013-45265-R, the INTERREG SUDOE program ECOAL-MGT, and in part by the Comunidad de Madrid under projects EDISON (CCG2014/EXP-072) and SINFOTON-CM:S2013/MIT-2790. The work of S. Martín-López was supported by the Spanish Ministry of Science and Innovation through a "Ramón y Cajal" Contract.

#231569 - $15.00 USD Received 16 Jan 2015; revised 23 Mar 2015; accepted 25 Mar 2015; published 14 Apr 2015